Characterization of a New Zinc Fixed-Point Cell for ITS-90 Realization

International Journal of Thermophysics (2022) 43:106
https://doi.org/10.1007/s10765-022-03032-x

Characterization of a New Zinc Fixed-Point Cell for ITS-90 Realization

G. Lopardo[1] · **R. Dematteis**[1] · **P. P. M. Steur**[1]

Received: 19 November 2021 / Accepted: 14 April 2022

Abstract
A new zinc fixed-point cell for the dissemination of International Temperature Scale (ITS-90) was realized at the Italian National Metrological Institute (Istituto Nazionale di Ricerca Metrologica, INRiM). This paper presents the results of its characterization, including fabrication details. In particular, immersion effects and influences of impurities on the freezing point of zinc were studied. The new open-type cell was prepared using a high purity sample, chemically analyzed, and the depression of the fixed-point temperature was calculated using the method of Sum of Individual Estimates (SIE). The new cell presents a smaller freezing point depression compared with the national reference for which the Overall Maximum Estimate (OME) method was applied. This behavior was confirmed also by the direct comparison of the two cells. These results provide confidence on the agreement between the experimental comparison and the SIE/OME evaluation. Finally, the improvement of the new zinc cell is reflected also in a lower uncertainty budget for the fixed-point realization.

Keywords Cells comparison · Chemical impurities · Fixed-point · Immersion profile · ITS-90 · Uncertainty · Zinc

1 Introduction

A fundamental task of a Primary Thermometry Laboratory is the realization of the International Temperature Scale (ITS-90) and the calibration of customers' standard thermometers at the defining fixed points [1]. Among the so-called metal fixed points is the freezing point of zinc (Zn). The way of realizing the fixed points in the range between − 38.8344 °C and 961.78 °C is described in [2]. Methods to estimate the influences of impurities on phase transition temperature were reported in various papers [3–5].

✉ G. Lopardo
g.lopardo@inrim.it

[1] Istituto Nazionale di Ricerca Metrologica - INRiM, Strada Delle Cacce, 91, 10135 Turin, Italy

Published online: 13 May 2022

During the last years, the attention of the thermometry community was focused on spurious immersion effects in zinc cells [6, 7]. In fact, due to radiative heat transfer phenomena, the temperature measured as a function of the height above the bottom of the re-entrant well, does not track the hydrostatic-head correction [2]. The immersion characteristic of a cell is strongly dependent on its design, assembly, furnace, SPRT, and also on plateau realization method [8].

At INRiM the current reference standard for the zinc freezing point is the cell Zn Co3. It was manufactured in the early 1990s at the Istituto Metrologico "Gustavo Colonnetti", IMGC (later INRiM), using a 99.9999 % pure zinc rod (produced by Cominco). In February 2018, a new zinc cell, called Zn JM1, was constructed. The higher chemical purity of the ingot (7N nominal purity) in comparison with the 6N nominal purity for cell Zn Co3 reduces the effects of impurities on the transition temperature bias. Therefore, the uncertainty of the fixed-point realization will improve with the use of the new cell.

This paper reports, in section 2, on the fabrication of the cell, while in section 3 are described the results of the characterization and immersion profile. Section 4 describes the comparison of the new cell with the national standard. Section 5 is devoted to the analysis of the influence of chemical impurities with different methods and the evaluation of the uncertainty budget for the fixed-point realization, while the conclusions are drawn in section 6.

2 Material and Methods

The cell Zn JM1 is constructed using a Zn sample (single ingot weighing 0.9595 kg) manufactured by Johnson Matthey (Lot No. M4282-3). The chemical analysis certificate from Azelis (Paris) confirms its nominal purity grade of 99.99999 %.

As recommended in the Guide to the Realization of the ITS-90 [2] the ingot is inserted in a cylindrical graphite crucible 220 mm long, 44.5 mm in external diameter, 35 mm in internal diameter. Ultra Carbon Division (USA) manufactured this crucible with a specific purification down to the 5 ppm level. This graphite exhibits a density of 1830 kg/m^3, a porosity of 10 vol %, and an average grain size of 10 µm. The same graphite was used for the construction of cell Zn Co3. Before inserting the metal, the crucible was submitted to a high-temperature cleaning treatment, heating it at 750 °C for 1 week in an argon atmosphere renewed several times with pure argon.

The crucible is capped with a graphite lid having a central hole allowing a graphite re-entrant tube of about 10 mm inner diameter to be axially located in the ingot. A closed borosilicate glass cell holder (460 mm long, 50 mm in external diameter, and 45.5 mm internal diameter) is used to surround the crucible. The thermometer well (external diameter 10 mm, and internal diameter 8 mm), put inside the crucible, is also made of borosilicate glass and its exterior sandblasted over its entire length. The overall depth of the re-entrant thermometric well from top to bottom is 470 mm.

The surface of the borosilicate glass cell holder and the thermometric well were cleaned in ultrasound with diluted acid (consisting of 12 % HF–40 %, 44 % HNO3–65 %, and 44 % deionized water) and then with deionized water.

In order to construct an open cell, the holder is sealed at the top with a stainless steel header, allowing the introduction of argon gas (nominally 101325 Pa) for thermal exchange and purging of possible impurities.

The zinc sample, supplied as a single rod still in its original plastic packing, was put inside the crucible. The dimensions of the ingot were as ordered on purpose to fit the crucible geometry.

After the insertion, the cell was subjected to the usual purging process with pure argon: the cell was first completely evacuated and then filled again with argon (101325 Pa), this procedure was repeated 3 times. Then the melting of the sample took place inside the crucible, still in argon atmosphere at a temperature of about 1.5 K above the melting point. Once this temperature was reached and the whole sample was melted, the well was pushed gently into the molten metal down to the point where about 1 cm of metal remained below the well. This operation was carried out under constant argon flushing.

On return to room temperature, the crucible was opened up for inspection of the surface. The metal showed a polished appearance over the first 4 cm of length, and a matted aspect on the rest. At this stage, the depth of the thermometer immersion was determined, for an accurate application of the immersion correction. The sample was then returned into the crucible, which on its turn was mounted into the cell holder with the thermometric well, covered with various layers of graphite rings and LoCon Felt Fiberfrax insulation. The internal space was then again flushed repeatedly with pure argon.

After the cell assembly, a series of Zn freezing plateaus were carried out in a potassium heat pipe furnace (ISOTECH model 17706) following laboratory procedure [9]. This procedure prescribes that after melting overnight to a uniform temperature about 4 K above the melting point, the temperature is slowly reduced by changing the set-point of the furnace controller to 2.5 K below the freezing point. When nucleation becomes evident by an initial arrest on the cooling curve, the thermometer is withdrawn from the well and an alumina rod is inserted for 1 min. This induces the growth of a mantle on the thermometer well, while the cooler furnace generates the other mantle. At this point, the set-point of the furnace is changed to about 0.5 K below the freezing point, in order to have long plateaus.

A primary resistance bridge (ASL model F18) coupled with an external 100 Ω standard resistor (Tinsley 5685A) placed in its temperature-controlled enclosures (Tinsley 5648) was employed to measure the thermometer resistance. The standard platinum resistance thermometer (SPRT) used was the model CHINO RS13 Z-02, applied as check thermometer for the Zn freezing point.

3 Results

Figure 1 displays the best freezing plateau obtained with Zn JM1 cell.

In the left part of the graph, we report the temperature variation (T-T_{max}) as a function of time, in the right part as a function of the inverse of the liquid fraction (F). T-T_{max} was evaluated starting from R-R_{max}, where R is the measured resistance and R_{max} is the resistance evaluated at $1/F$=1.5, where the peak of plateau occurs.

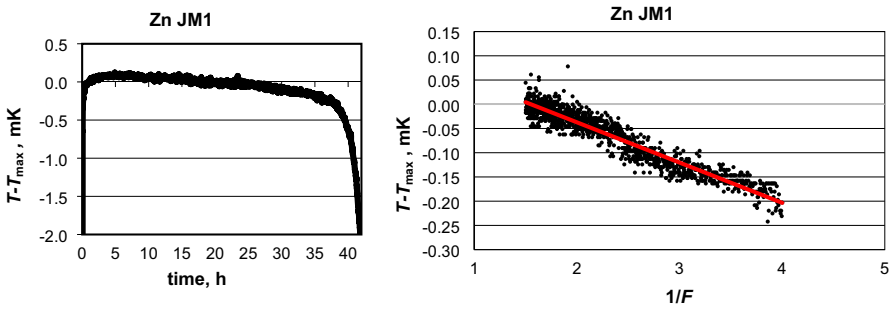

Fig. 1 A full freezing plateau for Zn JM1 cell. The temperature variation in function of time is reported in the left part, in function of $1/F$ in the right part. The furnace was set at 0.5 °C below the fixed-point temperature. Figure in color only online

Focusing on left part of Fig. 1, for about 30 hours the temperature was stable within 0.25 mK, and for about 40 hours within 0.6 mK.

A red straight line in the right part of Fig. 1, shows a linear trend of the plateau and its slope is reported. The slope is derived based on data at the range between $1/F$=1.5 and $1/F$=4.

During the transition of Fig. 1, the furnace was set to 0.5 °C below Zn fixed-point temperature. This set-point is considered to minimize the cell-furnace interaction. In order to evaluate the effect of heat exchange the transition was repeated at another set-point. In Fig. 2 we report the plateau obtained with the furnace at 1 °C below Zn fixed-point temperature. The value of $R_{\max}$ is the same as in Fig. 1.

The immersion profile on the plateau is reported in Fig. 3 together with the hydrostatic-head correction [2]. The immersion profile was measured inserting the thermometer starting at 8 cm from the bottom of the re-entrant tube, then inserting it at 6 cm, 4 cm, 2 cm, 1 cm and the bottom. This procedure was applied in order to avoid cold gas to be sucked in (as would happen with the commonly used opposite method), thus maintaining thermal equilibrium inside. Because of this consideration no attempt with the withdrawal method was made. At each position the self-heating correction was applied.

The behaviour is similar in magnitude and shape to that observed by other authors [10] in similar cells using a short thermometric well [6] and using an SPRT sandblasted on the exterior over its entire length (except in the part adjacent to the sensing element) [7].

The new cell was compared with the reference standard, Zn Co3, which participated in the following key comparisons: CCT-K3 [11], EURAMET.T-K3 [12], CCT-K9 [13] (in progress), EURAMET.T-K9 (in progress).

A phase transition obtained with Zn Co3 cell is reported in Fig. 4. The representation is in the style of Figs. 1 and 2.

Focusing on left part of figure, for about 30 hours, the temperature was stable to within 0.4 mK, a full melt was obtained after about 36 hours.

The immersion profile inside the Zn Co3 cell is not shown to preserve the blindness of CCT-K9 Key comparison, but, considering the measurement

uncertainty, the profiles inside the two cells are comparable. This behaviour was expected because the same cell geometry and furnace were employed for the measurements.

4 Comparison with the National Reference

After the first tests, we performed a direct comparison between the new Zn JM1 cell and the National reference Zn Co3. The measurements were done using two identical furnaces, where both cells were connected to the same gas system and pressure gauge, operating on both simultaneously. The plateaus in the two cells were induced at the same time using the same SPRT to measure temperature, switching quickly from one cell to the other and back again, while both were on plateau. Four rounds of assessments were performed in different days, and a new phase transition was induced every day in the cells. During each run, the transition temperature was determined several times for each cell, alternating the two cells in measurement. The measurement current was 1.414 mA and the self-heating effect was determined switching the current to 2 mA.

Given the experimental configuration, no significant differences in thermometer self-heating were encountered between the two cells.

Figure 5 reports the difference in transition temperature between cells Zn JM1 and Zn Co3 obtained for the different measurements carried out during the comparison. The transition temperature for Zn JM1 is found to be on average 0.29 mK higher than for Zn Co3 with a (purely statistical) standard deviation of 0.06 mK.

The higher transition temperature for cell Zn JM1 is evident also in Fig. 6 where the single resistance readings (R_0), reduced to 0 mA, are shown for the two cells.

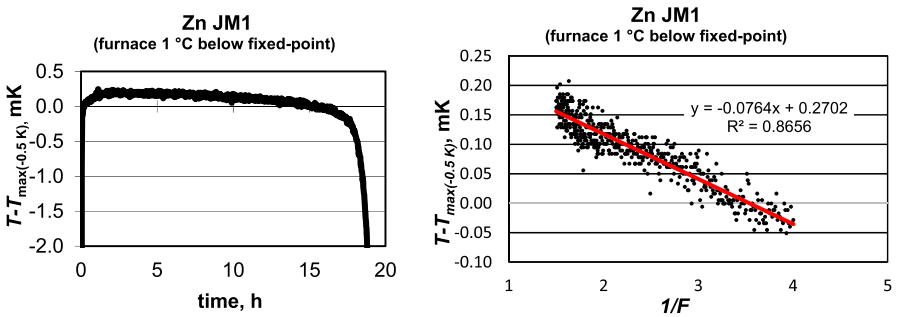

Fig. 2 A full freezing plateau for Zn JM1 cell. The temperature variation as a function of time is reported in the left part, as a function of $1/F$ in the right part. The slope is derived based on data at the range between $1/F = 1.5$ and $1/F = 4$. The furnace was set at 1 °C below the fixed-point temperature. Figure in color only online

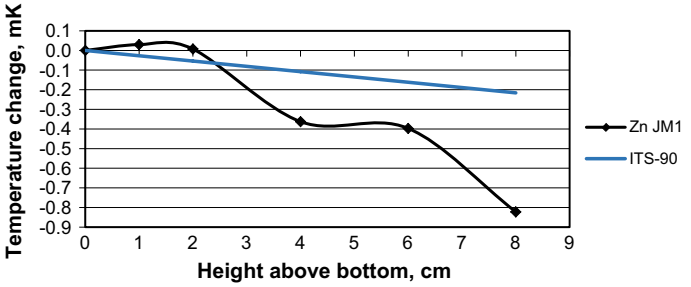

Fig. 3 Immersion profile of the SPRT inside the Zn JM1 cell during phase transition. The hydrostatic pressure line is also reported for comparison. The furnace was adjusted to 0.5 °C below fixed-point temperature. Figure in color only online

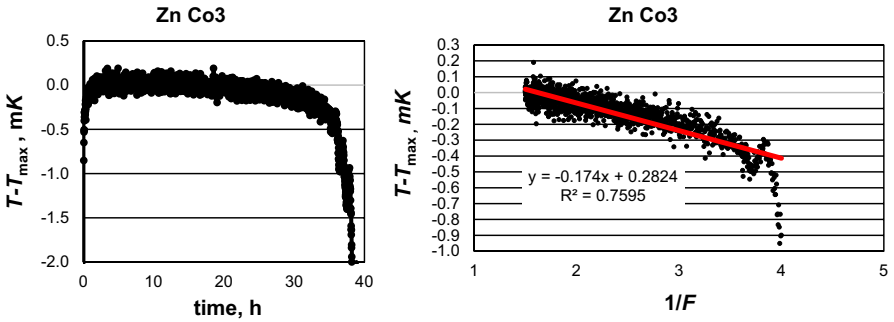

Fig. 4 A full freezing plateau for Zn Co3 cell. The temperature variation as a function of time is reported in the left part, as a function of $1/F$ in the right part. The slope is derived based on data at the range between $1/F = 1.5$ and $1/F = 4$. The furnace was set at 0.5 °C below plateau. Figure in color only online

5 Discussion

The results reported in previous sections show an improvement of the new cell Zn JM1 compared with Zn Co3, the National standard. In support of this statement, we have 2 pieces of evidence:

1. The results of the direct comparison, Figs. 5 and 6, show that the transition temperature in the cell Zn JM1 is 0.29 mK higher than in Zn Co3 with respect to the uncertainty of the comparison, which is 0.28 mK (in $k = 2$) as will be illustrated in Table 3.
2. The slope of the freezing curve of cell Zn JM1 is lower than for Zn Co3, as reported in Fig. 1 and 4 (right part), where that of cell Zn JM1 is 0.083 mK, while Zn Co3 is 0.174 mK

Considering the experimental setup and the uncertainties involved we tend to attribute the improvement of the new cell to the higher purity of the metal used [3].

With a direct cell comparison alone, it is not possible to quantify experimentally the effect of impurities on freezing point temperature because the method depends

strongly on the reference cell and plateau realization procedure [14]. Other methods, such as the Sum of Individual Estimates (SIE) or the Overall Maximum Estimate (OME) [3], are more meaningful because they directly link the temperature depression to chemical impurity content. However, a cell comparison can be considered a useful method to validate the quality of the cell. Its advantage is to reflect accurately the difference in the impurity content of the ingot while keeping under control other possible causes that could determine a temperature shift such as limitations of the chemical analysis, contamination of the material during the cell preparation, etc.

In this paper, the SIE method was adopted to estimate the uncertainty component due to impurity content for Zn JM1 cell. This method is used when sufficient chemical analysis information is available.

The SIE approach uses Eq. 1 for the change in the observed fixed-point temperature (T_{obs}) relative to that of the chemically pure material (T_{pure}) at the liquidus point [4].

$$\Delta T_{\mathrm{SIE}} = T_{pure} - T_{obs} = -\sum_{i} c_{\mathrm{li}} m_{\mathrm{li}} \tag{1}$$

c_{li} is the concentration of the impurity i at the liquidus point, and $\mathrm{m_{l1}}$ the liquidus-line slopes for each chemical impurity [15]. The summation is over all impurities present in the liquid.

Table 1 reports the data and result for the Zn batch employed for the new cell Zn JM1. The element concentrations reported in the chemical analysis certificate were obtained by GDMS technique. The detection limit is 1 ppb, and the impurity concentration limit is between 2 ppb and 5 ppb.

The total impurity concentration calculated in Table 1 is in accordance with the 7N nominal purity grade declared. The depression of the freezing point temperature, relative to that of the pure metal (419.527 °C) is equal to 0.017 mK.

The standard uncertainty of the estimate ΔT_{SIE} results from the uncertainties of the analysis results $u(c_{\mathrm{li}})$ and the data for the concentration dependences $u(m_{\mathrm{li}})$, as reported in Eq. 2

$$u^2(\Delta T_{\mathrm{SIE}}) = \sum_{i} \left[u\left(c_{\mathrm{li}}\right) * m_{\mathrm{li}}\right]^2 + \left[c_{\mathrm{li}} * u(m_{\mathrm{li}})\right]^2 \tag{2}$$

where $u(m_{\mathrm{li}})$ was evaluated considering 30 % uncertainty in liquidus slopes, as suggested by Pearce et al. in [15] and $u(c_{\mathrm{li}}) = c_{\mathrm{li}}$ as suggested by da Silva et al. in [5].

As stated by Fellmuth and Hill [4] impurities with concentration below the detection limit are omitted from the correction to the temperature of the fixed-point but are included in the standard uncertainty (with half the detection limit used as the standard uncertainty of the concentration).

The standard uncertainty for the correction is equal to 0.006 mK [5]. Summing in quadrature with the value from the detected components, an overall value of 0.018 mK is obtained as the uncertainty.

Instead, for the cell Zn Co3, the Overall Maximum Estimate (OME) method was applied for evaluating impurity effects. In fact, being an old cell, a chemical analysis certificate is not available and the exact concentration of each element is not known.

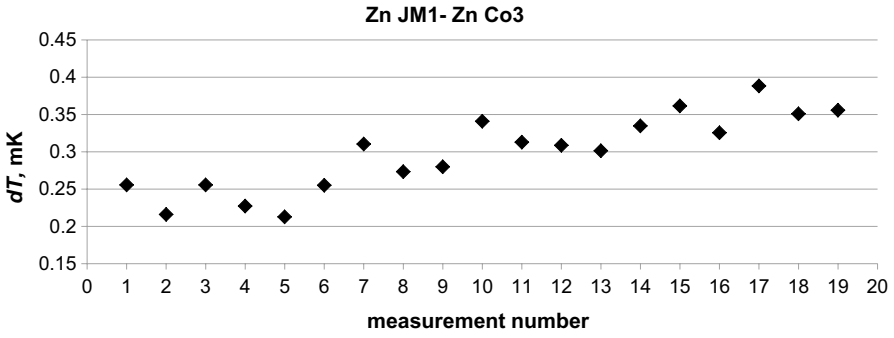

Fig. 5 Difference in transition temperature between cells Zn JM1 and Zn Co3. The x-axis represents the progressive measurement sample

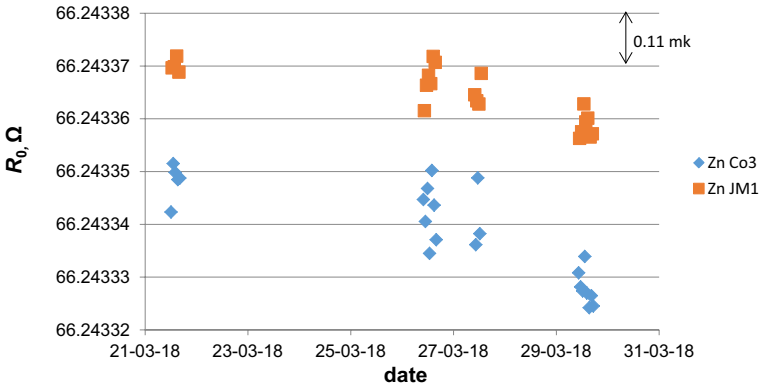

Fig. 6 R_0 measured for cell Zn JM1 and Zn Co3 during different days from March 21st to March 29th 2018. Figure in color only online

In this case, all that is required is an estimate of the overall impurity concentration, expressed as a mole fraction. With this, the OME for the liquidus point temperature change is given by [3]:

$$\Delta T_{OME} = c_{l1}/A \tag{3}$$

A is the first cryoscopic constant, that for Zn is equal to 0.001772 K^{-1} [16], and c_{11} is the total impurity concentration when the fixed-point material is completely melted. In the case of Zn Co3 sample c_{11} is equal to 10^{-6} and Eq. 3 gives a depression in freezing temperature of 0.56 mK, based on the nominal purity and thus to be regarded as a maximum limit.

These results were used to evaluate the uncertainty component arising from the impurity content.

For Zn JM1 the standard uncertainty is set equal to 0.018 mK. The Guide to the ITS-90 [3] recommends the application of a correction for the known impurity effect

Table 1 Coefficients employed in Eq. 1 for cell Zn JM1

Element	c_l	m_i	$c_{li}m_{li}$
	ppm	mk/ppm	mk
Cu	0.001	0.27	0.00027
Ag	0.001	0.3	0.0003
Mg	0.0025	− 1.03	− 0.002575
Sb	/	− 0.33	/
Ni	0.0025	− 0.6	− 0.0015
Co	0.0025	− 0.61	− 0.001525
Bi	/	− 0.14	/
In	0.0025	− 0.38	− 0.00095
Ca	/	2.42	/
Fe	0.005	− 0.58	− 0.0029
Cd	0.01	− 0.34	− 0.0034
Cr	/	− 1.64	/
As	/	− 0.46	/
Si	/	− 1.28	/
Al	0.0025	− 0.92	− 0.0023
Se	/	− 0.23	/
Pb	0.0025	− 0.49	− 0.001225
Sn	0.0025	− 0.31	− 0.000775
Total concentration	**0.069**	$\Delta T_{SIE} = -\sum_i c_{li}m_{li}$	**0.01658**

c_l is the concentration of the impurity i at the liquidus point. m_i is the liquidus-line slopes for each chemical impurity (the data have been taken from [15]). The result for ΔT_{SIE} is reported, and also the total concentration of impurities

and entering only the uncertainty deriving from the effect into the uncertainty budget. However, considering the very small entity of the effect for Zn JM1 with respect to the overall uncertainty budget, it was decided, for practical reasons, to enter it in the uncertainty budget instead of applying a correction for the effect.

For Zn Co3, it is assumed that any liquidus temperature from $-\Delta T_{OME}$ to zero is equally likely, i.e. a rectangular distribution, thus the standard uncertainty (u_i) is equal to

$$\frac{\Delta T_{OME}}{\sqrt{3}} = -0.32\text{mK}$$

The complete uncertainty budget for the realization of the Zn fixed-point for the two cells is reported in Table 2. The first block ("Cell") is related to cell fabrication and it includes the following terms:

- "Gas pressure": is due to the effect of pressure on zinc fixed-point and it was evaluated considering the resolution and drift of the pressure gauge.

- "Variability of the plateau realization": accounts for the differences between the fixed-point temperature evaluated through repeated plateaus. It is the mean value of the differences between a plateau and another obtained in the following days.
- "Hydrostatic head" accounts for the hydrostatic pressure effect on the equilibrium temperatures, taking into account only the vertical dimensions, with an overall uncertainty of 0.5 cm.
- "Heat flux-immersion error" was obtained recording two plateaus at different furnace temperatures, 0.5 °C and 1 °C below zinc freezing point. The maximum of transition temperature was evaluated through linear regression, for the two set points and their difference calculated. A rectangular probability distribution was assumed.
- "Slope of the plateau" is the uncertainty component linked to the variation of temperature measured during a day long comparison. In other words, it is the mean difference, for each zinc cell, between the first measurement and the last in the same day. A rectangular probability distribution was assumed.

The second block ("Resistance Measurements") reports the terms related to the measurement system. "Reference resistor stability" considers the effects of slight temperature variations of the standard resistor. Finally, the "thermometer self-heating" term reflects the uncertainty in the extrapolation of the SPRT resistance to zero current. This was evaluated as the standard deviation of the self-heating measured in each cell during the fixed-point temperature determination.

Based on these calculations, the new cell allows us to reduce the expanded uncertainty for the Zn fixed-point realization to 0.28 mK (instead of 0.69 mK for cell Zn Co3).

Regarding the direct comparison of the two cells, its uncertainty is evaluated equal to 0.28 mK as reported in Table 3.

6 Conclusion

A new Zn fixed-point cell, named Zn JM1, was realized at INRiM using a batch of a purer material (7N) compared with the national standard Zn Co3 (6N). The new sample was initially intended to be used as a working standard, but after its characterization, the intention is now to substitute the national standard.

The influence of impurities on the fixed-point temperature, for the new cell, was evaluated to be equal to 0.017 mK with the SIE method, due to a sufficiently detailed chemical analysis certificate being available for the metal. Instead, for the old reference cell the influence of impurities is equal to 0.56 mK, where the OME method was applied because the chemical analysis certificate was not available. Considering the very small entity of the correction, it was decided to enter it into the uncertainty budget, instead of applying it explicitly as a correction, as recommended by the ITS-90 Guide. This argument is supported also by the overall uncertainty of the correction obtained by SIE method (0.018 mK) being almost equal to the correction itself.

Table 2 Uncertainty budget for the realization of the Zn fixed-point for cell Zn JM1 and Zn Co3

Source of uncertainty	Contribution to the combined standard uncertainty/mK	
	Zn JM1	Zn Co3
Cell		
Chemical impurities	0.018	0.32
Gas pressure	0.03	0.03
Variability in plateau realization	0.10	0.08
Hydrostatic head	0.01	0.01
Heat flux – Immersion Error	0.05	0.01
Slope of plateau	0.02	0.04
Resistance Measurement		
Bridge repeatability	0.02	0.02
Bridge non-linearity	0.02	0.02
Bridge quadrature effects	0.02	0.02
Reference resistor stability	0.01	0.01
Thermometer Self-heating	0.06	0.07
Combined standard uncertainty, ($k = 1$)	**0.14**	**0.34**
Expanded uncertainty ($k = 2$)	**0.28**	**0.69**

This improvement was also confirmed by experimental data. In fact, Zn JM1 presents a flatter freezing plateau than Zn Co3 cell. Besides, the direct comparison between the two cells showed that the mean transition temperature for Zn JM1 is 0.29 mK higher than for Zn Co3 with uncertainty of 0.28 mK, in k=2.

The difference evaluated experimentally (0.29 mK) is half the difference, in mK, of the temperature depression between cell Zn JM1 and Zn Co3 calculated from their impurity content, suggesting substantial agreement between the comparison to the SIE/OME evaluation, with OME yielding only a maximum limit.

Besides, these evidences indicate that the contamination of the metal during the filling process was kept to a minimum or virtually did not occur in a manner to affect the phase transition temperature of the cell.

Finally, significant spurious radiative heat transfer effects were not evident in the immersion profile.

The complete uncertainty budget for the realization of the Zn fixed-point shows a significant reduction in comparison with the actual reference standard. This will allow a reduction of the laboratory Calibration and Measurement Capabilities (CMCs) for the calibration at ITS-90 fixed points of cells and standard platinum resistance thermometers.

Table 3 Uncertainty budget for the comparison of the Zn fixed-point cells Zn JM1 and Zn Co3

Source of uncertainty	Contribution to the combined standard uncertainty/mK
Standard deviation of the comparison	0.06
Resolution of the pressure gauge	0.01
Variability in plateau realization	0.10
Bridge repeatability	0.02
Reference resistor stability	0.01
Thermometer Self-heating	0.07
Combined standard uncertainty, ($k = 1$)	**0.14**
Expanded uncertainty ($k = 2$)	**0.28**

Declarations

Conflict of interest The authors declare that they have no conflict of interest.

Ethical Approval Not applicable.

References

1. H. Preston-Thomas, Metrologia **27**, 3–10 (1990). https://doi.org/10.1088/0026-1394/27/1/002
2. Guide to the Realization of the ITS-90 Fixed Points: Metal Fixed Points for Contact Thermometry (2018) https://www.bipm.org/utils/common/pdf/ITS-90/Guide_ITS-90_2_4_MetalFixedPoints_2018.pdf. Accessed June 2020
3. Guide to the Realization of the ITS-90 Fixed Points: Influence of Impurities (2018) https://www.bipm.org/utils/common/pdf/ITS-90/Guide_ITS-90_2_1_Impurities_2018.pdf. Accessed June 2020
4. B. Fellmuth, K.D. Hill, Metrologia **43**, 71–83 (2006)
5. R. da Silva, J.V. Pearce, G. Machin, Metrologia **54**, 365–380 (2017)
6. S. Rudtsch, A. Aulich, C. Monte, Temperature: its measurement and control in science and industry, volume 8. AIP Conf. Proc. **1552**, 265–270 (2013). https://doi.org/10.1036/1.4819551
7. J.V. Pearce, J. Gray, R. Veltcheva, R. Da Silva, Meas. Sci. Technol. **30**, 124001 (2019)
8. G.F. Strouse, Tempmeko '99: the 7th Int. Symp. on Temperature and Thermal Measurements in Industry and Science ed. J.F. Dubbledam and M J de Groot (Delft: NMi-Van Swinden Laboratorium) pp. 147–52 (1999)
9. P. Marcarino, P.P.M. Steur, R. Dematteis, Temperature, its measurement and control in science and industry. AIP Conf. Proc. **684**, 65–70 (2003)
10. R. da Silva, J. Pearce, Metrologia **58**, 015003 (2021)
11. B.W. Mangum et al., Metrologia **39**, 179–205 (2002)

12. E. Renaot et al., Int. J. Thermophys. **29**, 991–1000 (2008). https://doi.org/10.1007/s10765-008-0397-x
13. P.P. M Steur, R. Dematteis, INRiM Internal Report N°14/2018 (April)
14. J.V. Widiatmo, K. Yamazawa, J. Tamba, M. Arai, Direct Cell Comparison for Evaluation of Impurity Effect in Fixed-Point Realization, BIPM Com. Cons. Thermométrie 25, Document CCT/10–22 (2010) https://www.bipm.org/cc/CCT/Allowed/25/D22_Direct_Cell_Comparison_(NMIJ)_revised.pdf. Accessed July 2020
15. J.V. Pearce, J.A. Gisby, P.P.M. Steur, Metrologia **53**, 1101–1114 (2016)
16. S. Rudtsch, Cryoscopic Constant, Heat and Enthalpy of Fusion of Metals and Water. BIPM Com. Cons. Thermométrie 23, Document CCT/05–04/rev (2005). http://www.bipm.org/cc/CCT/Allowed/23/CCT_05_04_rev.pdf. Accessed July 2020